Coastal Dynamics 2017
Paper No. 058

Periodic saltation under extreme tidal currents: an experimental study

Gaspard Minster[18], France Floc'h[2], Alexandre Valance[3], Nicolas Le Dantec[24], Amandine Nicolle[15], Olivier Blanpain[6], Jean-François Filipot[7], Benoit Zerr[18]

Abstract

In extreme tidal environment and specifically in the Alderney race (English Channel, France), the ambition to install hydrokinetic turbines requires knowledge on the pebbles concentration in the water column. Some evidences of the presence of such coarse sediments at one meter above the bed have been found. An experimental study is realized in a free surface flume for high Stokes number. With fast camera the trajectories of hundreds of spherical particles are analyzed. This study focuses on the characterization of the critical Shields number to intermittent and saltation regime and on the coefficient of restitution between the impact and the rebound velocity. The critical Shields number is identified experimentally at 0.2. The restitution coefficient shows little dependence on the impact angle. Finally, the experimental maximum height reached by the spherical particles proves that lift and inertia forces are not negligible.

Key words: Saltation, hydrodynamics, Experimental modelling, Shields number, Restitution coefficient, High Stokes number

1. Introduction

Hydrokinetic turbines must be deployed under strong currents where sediment transport can be important. The three-year project PHYSIC (2016-2019) focuses on sediment dynamics in the Raz-Blanchard (Alderney race, English Channel). This environment experienced one of the strongest tidal currents in the world. Evidences of pebbles (diameter ~ some cm) jumps at tens of centimetres high have been obtained during previous field campaigns. This coarse particle flux may represent a constraint for the scaling of hydrokinetic turbines. However, until now, the potential danger of the coarse particles load over the turbines was not taken into account. This study focuses on the pebbles dynamics under extreme tidal current and in particular on the saltation regime. This regime might allow particles to reach a significant height in the water column, and thus may cause damages to the immerged turbines and associated devices.
Despite several decades of investigation on sediment dynamics, transport calculation largely relies on empirical formulations (Soulsby (1997), Van Rijn (1984)), and a complete description of the processes for extreme flow conditions and coarse particles is lacking (Van Rijn (1993), Niño & García (1998).). Continuing saltation regime is studied numerically for aeolian and aquatic environment by Jenkins et al (2014) and Berzi et al. (2016). While aeolian particles reach a saltation regime for low Shields number, high Shields number are required for achieving continuing saltation in aquatic environment. However, Berzi et al. (2016) suggest that at lower Shields number, a rolling regime or intermittent saltation takes place where turbulent burst may play an important role as emphasized in Blanpain (2009). Williams (1990) observed that 60% of the total horizontal flux was due to turbulent bursts events, which occur during 24% of time.

[1] ENSTA-Bretagne, OSM, 2 rue François Verny, BP 92208, 29806 Brest cedex 9, France.
gaspard.minster@ensta-bretagne.fr; amandine.nicolle@ensta-bretagne.fr; benoit.zerr@ensta-bretagne.fr
[2] Domaines Océaniques UMR 6538, UBO/IUEM, France france.floch@univ-brest.fr
[3] CEREMA, DTecEMF, F-29280 Plouzané,France nicolas.ledantec@univ-brest.fr
[4] Institut de Physique de Rennes alexandre.valance@univ-rennes1.fr
[5] Station Biologique de Roscoff, Laboratoire Adaptation et Diversité en Milieu Marin (AD2M), UMR 7144
[6] SHOM, olivier.blanpain@shom.fr
[7] France Energie Marine, Jean.Francois.Filipot@france-energies-marines.org
[8] Lab-STICC,UMR CNRS 6285, Brest France

In this study, in order to get a deeper understanding of the intermittent saltation motion, an experimental study in a flume has been performed. The relationship between the height and the length of the jumps is characterised. The coefficient of restitution and its dependence to the impact angle are investigated. The height reaches by the particles is finally discussed according to analytical height calculated considering only the particles weight. The relative contribution of each force is estimated and a comparison to the numerical model of Berzi et al. (2016) is presented.

2. Experimental setup

2.1 Description of the device

In order to study the height, length of jumps, impact and rebound velocities and angle of saltated pebbles, experiments are carried out in a free-surface flume (figure 1) (40 cm wide, 60 cm height and 500 cm long). The flume is equipped with two pumps (figure 2) able to produce a flow discharge of 40 l/s. In theory, the maximal discharge is equal to 80 l/s but in practice, the maximal value is 65 l/s. To provide a parallel flow, the flume is constructed with a honeycomb, which is positioned between the pumps and the start of the flume. The honeycomb breaks the large turbulent structures. A difference of height between the flume and the pump allows limiting the vacuum effect generated. The flume can be inclined up to 10°. This inclination permits to increase the maximal velocity produced in the flume. In this study, the inclination remains close to 0°.
To empirically model the saltation effect, we have to create a roughness on which the particles could start to jump. If the roughness is too small, the particles keep on rolling on the bed. If the roughness is too big, the particles are trapped. We model the roughness with specific size of spherical particles (1.2 cm) pasted on two steals plate of one meter-long each. The uniform spatially roughness bed must be simulated with high surface fraction of particles to not create hole in the scheme, to have a dense packing bed respecting at the same time a non-crystalline structure. The two plates are then introduced in the flume at 2.5 meters from the honeycomb. In this way, the perturbation of the beginning and the end of the flume are maximally avoided.
The value of velocity in a free surface flume with a flat rough bed can be deduced analytically:

$$U(y) = \frac{u^*}{\kappa} ln\left(\frac{y}{y_0}\right) \quad (1)$$

Where u^* is the friction velocity, y_0 the hydraulic roughness and κ the constant of Von Karman. The roughness is defined according to the stuck particles diameter d following Nikuradse formula (VanRijn (1984a)) (y_0 equal to d/30=0.012/30).

Figure1. *Left* The flume of the IPR (Institute of Physics of Rennes); *Right* the velocity probe on the rough bed.

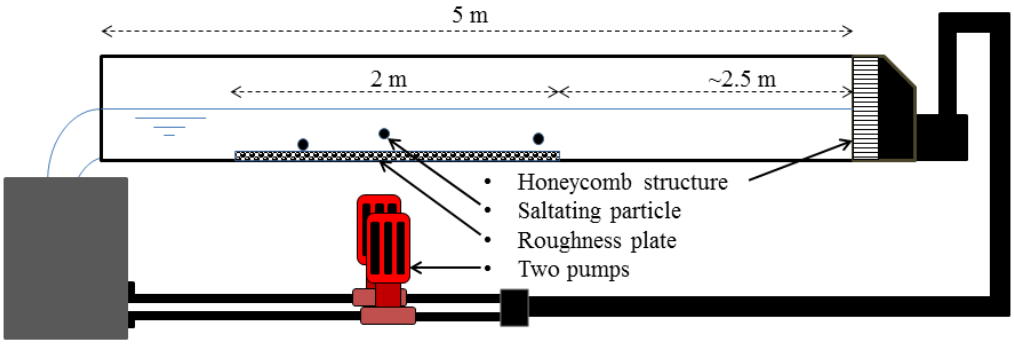

Figure2. Scheme of the flume of the IPR (Institute of Physics of Rennes)

The velocity profile is acquired on a vertical profile with a streamflow velocity meter model 403 from the enterprise Nixon (figure 1 *Right*). Hydraulic circuit requires less than 10 minutes in order obtaining a steady flow in the flume. Then the velocimeter is installed in the flow. It uses a little propeller of 11.6 mm diameter to measure the flow velocity according to its rotation speed. Six measurements are done at six different vertical positions (with 1 or 2 mm accuracy) in the middle of the flume. The instrument gives us a 10s averaged flow data. The mean of thirty measurements (5 min) is used as the mean flow velocity at the considered vertical position and the uncertainties on the value corresponds to the standard deviation. The vertical profiles measured with the rough bed allow us to compute the Shields number in the flow and a comparison to the analytical profile is also performed (figure 3). With the surface velocity measured, the value of u^* can be established with equation (1). The threshold bed shear stress τ_{cr} is next established from the equation:

$$\tau_{cr} = \rho^f \, u^{*2} \tag{2}$$

With ρ^f the fluid density, and from this value the Shields number Sh is obtained through:

$$Sh = \frac{\tau_{cr}}{g(\rho^s - \rho^f)d} \tag{3}$$

With ρ^s the mass density of the particle, d the diameter of the particle, μ^f the molecular viscosity of the fluid and g the gravitational acceleration.

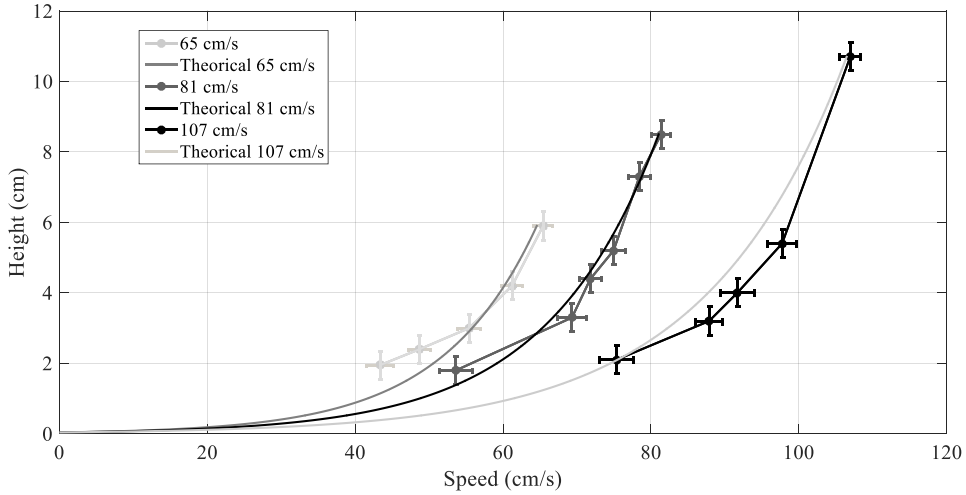

Figure 3. Velocity profiles of the flow for three prescribed flows: 11l/s, 24 l/s and 54 l/s and the corresponding analytical logarithmic profiles. The data are characterized by the maximal velocity assimilate to the surface velocity. The origin of the vertical axis corresponds to the surface under the roughness represented by particles of 1.2 cm diameter.

Figure 3 shows the vertical velocity profiles acquired for three prescribed flows. The maximum velocity is obtained 2 cm under the surface (highest point of figure 3 profiles) and is considered as the surface velocity V_S. The surface velocities 65 cm/s, 81 cm/s and 107 cm/s correspond to prescribed flows of 11 l/s, 24 l/s and 54 l/s respectively. In the following, the different experiment configurations are referenced according to the surface velocities. The Shields number for each configuration is calculated from the logarithmic shape of the corresponding analytical curve. Results are summarized in Table 2.

2.2 Protocol

Nine cases are modelled in the flume with a 1.2 cm roughness: the trajectories of spheres of three different diameters (1.6 cm, 3 cm and 5 cm) for three different flows (11 l/s, 24 l/s and 54 l/s) are recorded. The fall particle Reynolds number and Stokes number (which characterizes the magnitude of the particle inertia in comparison with the viscous force) are defined as:

$$Re = \rho^f \frac{d^{3/2}}{\mu^f} \sqrt{\frac{g(\sigma - 1)}{\sigma}} \tag{4}$$

$$St = \sigma Re \tag{5}$$

With $\sigma = \rho^s/\rho^f$, the density ratio. The values of Re (Equation 4) are calculated with $\mu^f = 0.001$ Pa.s, $\rho^f = 998.2\ kg.m^3$ and $\sigma = 2.5$ for particles diameters of 3 and 5 cm and 2.47 for the 1.6 cm-diameter particles. This leads to the values: Re= 5.10^3 and St= 1.10^4 for d=1.64 cm; Re=1.10^4 and St=3.10^4 for d=3 cm and Re= 3.10^4 and St=7.10^4 for d=5 cm. These values for Stokes and Reynolds confirm that we are in the turbulent inertial regime.
The spheres are then released 5 by 5 into the flume via a gutter far enough from the measurement zone in order to reach a steady state of motion. To prevent initial jump on the gutter, a flexible surface in the back of the gutter is put. Thanks to this configuration, particles are introduced with only the speed induced by the current.

Trajectories of spheres are then recorded via high frequency camera to obtain a two dimensional representation. The acquisition frequency is 500 frames per seconds and the resolution varies from 1280 / 248 to 1280/ 400 pixels. The parameters have been chosen to have the best detection with the file size as small as possible.
Some tests have been performed with the camera in vertical position. The aim was to evaluate the deviation of the particle in the horizontal plane. 3D trajectories have not been computed because the vertical trajectory and the horizontal deviation have not been recorded at the same time. The horizontal deviation ratio is calculated as the ratio between the cumulated length covered by the particle perpendicularly to the flow direction and the length of the flume parallel to the flow direction.

2.3 Particle tracking

The free software Tracker is used to extract the position of the spheres on each image (see figure 4). A semi-automatic method is used in order to extract the position of each rebound on the bed. The horizontal distance between two rebounds give the length of the jump L. The difference between the maximum vertical position and the position on the bed at the previous impact gives the height of the jump H. The impact and rebound velocities are computed from the average on five values of velocities extracted from the software before and after the jump respectively. In this way, the problems of detection of the impact time step are avoided. The impact angle θ is defined as $\theta = \tan^{-1}\frac{V_{iy}}{V_{ix}}$ with V_{iy} and V_{ix} the vertical and horizontal component respectively of the impact velocity.
Two regimes of motions are identified: saltation and rolling. The motion is identified as rolling if the jump height is less than the roughness length. In such case, the sphere rolls on the bed roughness and no real jumps can be identified. A time ratio of rolling is computed for each configuration.

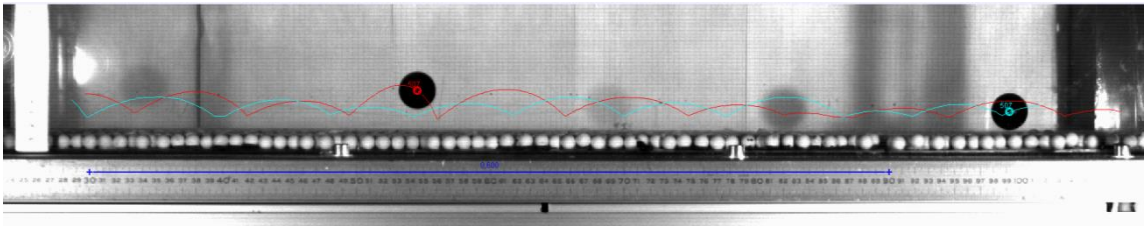

Figure 4. Screen shot of the acquisition of two 3 cm diameter particles in the flume superimposed with the two final trajectories processed. The bed of roughness is 1.2 cm; the direction of the flow is from the right to the left with a surface velocity of 107 cm/s.

3. Results analysis

Two different motion regimes are observed: rolling and saltation. In table 2 the rolling ratio decreases with increasing velocity flow and with decreasing sphere diameters. For the flow V_S = 65 cm/s, the particles of 3 and 5 cm never reach the saltation regime. If considering intermittent regime between 75% and 25% of rolling, the boundary with saltation regime (for 25% or less rolling motion) is about a Shields number of 0.1 for Stokes number between 10^4 and 10^5.

Table 1. Rolling ratio according to the particles diameter and the surface velocities

Surface velocity (m/s) / Particle diameter (cm)	0.65	0.81	1.07
1.6	23.2%	10.4%	4.8%
3	100%	16.0%	5.2%
5	100%	35.5%	12.2%

The percent of horizontal deviation is estimated at 9.8% at low speed ($V_S = 65$ cm/s) for spherical particles of 1.6 cm diameter, thus when the deviation may be maximum. The measure was realised on 28 cm long of flume considering 25 particles. This low ratio confirms that the motion is essentially in the flow direction.

The shape of histograms of length and height of jumps for each configuration is checked in order to justify a relevant statistic. An example for a surface velocity V_S of 107 cm/s and particles diameter of 3 cm is given on figure 5 for 1181 recorded jumps. Below 300 recorded jumps the results look like a stochastic distribution. Number of jumps and number of trials recorded for each configuration is given in Table 2. According to these distributions, the mean parameter and the standard deviation are computed and reported in Table 2. Higher the surface velocity, higher the mean jump heights and length. The small particles jump higher than the big particles, with 1.6 cm spheres jumps heights twice the 5 cm spheres jumps heights. The influence of the diameter on the jumps lengths is unclear. The standard deviation on the jumps lengths is between 20 and 50%. The standard deviation on the jumps heights is more than 50%.

In order to investigate the influence of motion properties such as impact or rebound velocities, or impact angle on the height and length of jumps, we focus in the following on each individual jumps. The estimation of the length of the jumps has a precision of ±0.5 mm. The error on the time is negligible, leading to an uncertainty on the velocity of the order of the cm/s. Figure 6 presents the height of the jump of the particle versus the length of the jump. Experiments performed for the same flow velocity are in the same color. Darker colors represent smaller spheres. The trends observed with the mean values are confirmed here: bigger the height bigger the length of the jumps and higher the discharge, bigger the length and height of jumps. The influence of the diameter is less obvious here.

Figure 6 shows that for each configuration a good linear fit can be obtained between the height and the length of the jumps. Defining the aspect ratio of the trajectory as H/L, this means that the aspect ratio may

tend to be constant for each configuration. More particularly, the surface velocity seems to be of higher importance than the diameter of the particle to determine the aspect ratio with H/L about 10, 5 and 3 for V_S = 107, 81 and 65 cm/s respectively. The aspect ratio increases faster than the surface velocity. In comparison the aspect of the curve seems less impacted by the diameter of the particle.

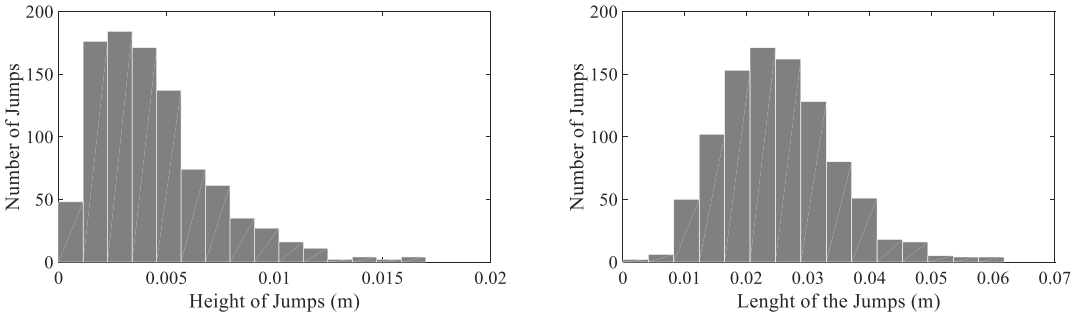

Figure 5. Histograms of distribution of the heights (*Left*) and the lengths (*Right*) of jumps for a surface velocity of 0.81 m/s and a particle diameter of 3 cm.

Table 2. Experimental data

Size of particle in movement (cm) d / Surface Velocity (m/s) Vs	Number of Trials	Number of recorded jumps	Shields Number	Mean Length (cm)	Standard deviation on Length (cm)	Mean Height (cm)	Standard deviation on Height (cm)
1.6 / 0.65	26	487	0.22	1.3	0.6 (46%)	0.35	0.20 (57%)
3 / 0.65	-	-	0.11	-	-	-	-
5 / 0.65	-	-	0.07	-	-	-	-
1.6 / 0.81	94	1455	0.26	4.9	1.9 (39%)	1.10	0.59 (53%)
3 / 0.81	52	1181	0.14	2.5	0.9 (36%)	0.44	0.28 (63%)
5 / 0.81	37	745	0.08	3.1	0.9 (29%)	0.40	0.22 (55%)
1.6 / 1.07	68	645	0.33	7.1	2.8 (39%)	1.34	0.77 (57%)
3 / 1.07	84	966	0.18	7.0	3.8 (54%)	1.10	1.00 (91%)
5 / 1.07	72	889	0.11	6.7	1.8 (27%)	0.66	0.42 (63%)

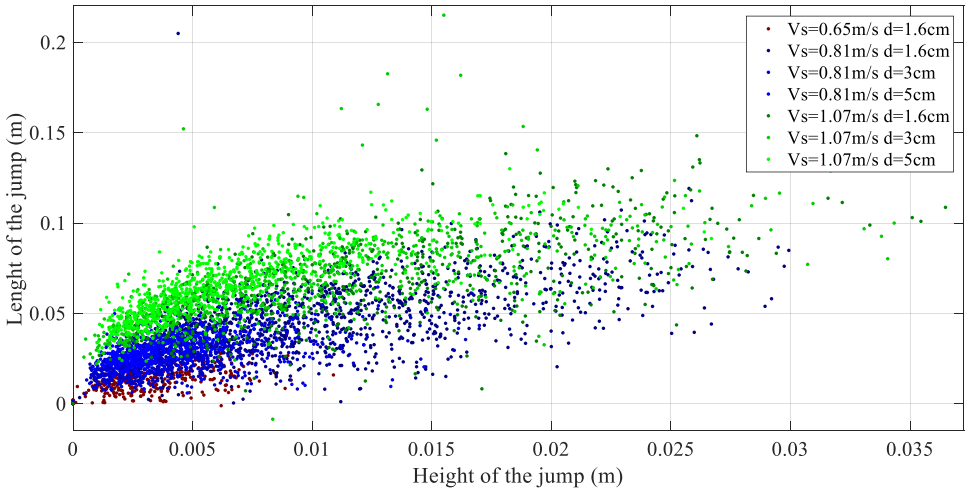

Figure 6. Height vs length of the jumps for seven configurations detailed in the legend according to the surface velocities Vs and particle diameters d

According to the studies of Beladjine et al. (2007), Crassous et al. (2007) and Oger et al. (2005) with experiments and numerical analysis, the particles rebounds on a bumpy bed follow a law of restitution after the impact depending only on the angle of the impact in case of Stokes number higher than 100. This law determines the rebound velocity according to the impact velocity. According to the velocities magnitudes, the restitution coefficient is given by:

$$e = a - b \times \sin(\theta) \tag{6}$$

and for the vertical direction:

$$-e_y = \frac{-a_y}{\sin(\theta)} + b_y \tag{7}$$

With a, b, ay, and by constant parameters. Beladjine et al. (2007) under high speed collision (26 m/s) in the air have obtained empirically: $a = 0.87, b = 0.72, a_y = 0.30$ and $b_y = 0.15$. θ is the impact angle (with the horizontal) defined previously.

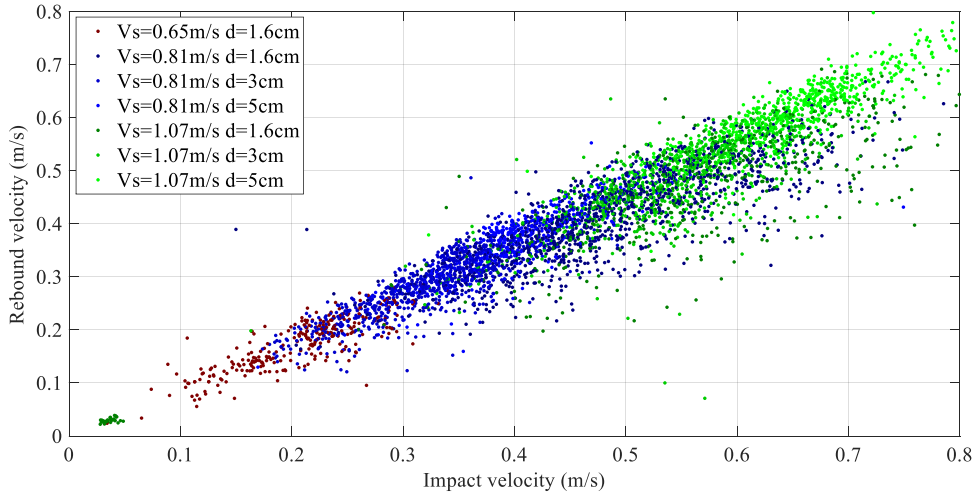

Figure 7. Rebound velocity vs impact velocity in order to determine the coefficient of restitution e for the seven configurations according to different surface velocities Vs and particle diameters d

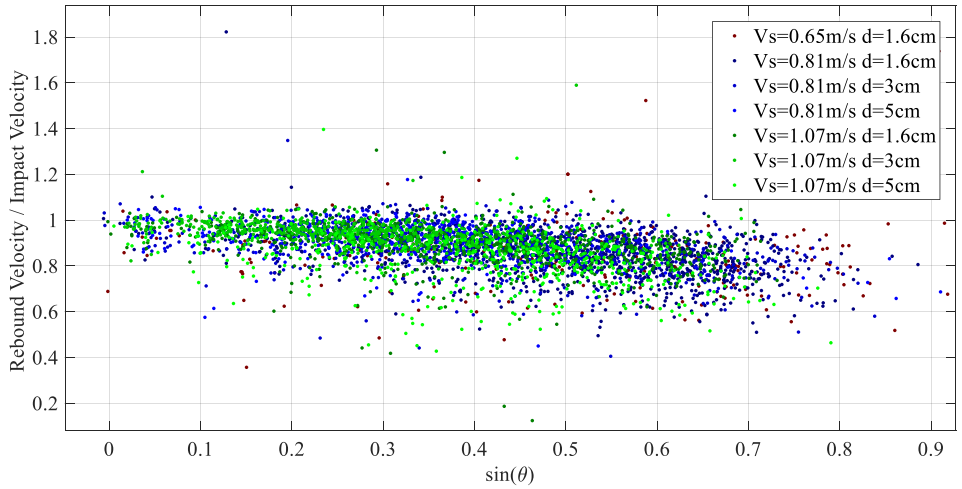

Figure 8. Restitution coefficient vs $\sin(\theta)$ for the seven configurations considering different surface velocities Vs and particle diameters d

The figures 7, 8 and 9 and the Table 3 represent the relation between the different parameters in order to determine the expression of the restitution coefficient. In the figure 7, the magnitude of the rebound velocity is shown to be directly proportional to the magnitude of the impact velocity. The coefficient of restitution is first assimilated to the slope of the linear fit thus as a constant. The resulting restitution coefficients are summarized in Table 3. The correlation is quite good considering the R^2 between 0.7 and 0.9. The mean coefficient is equal to 0.82 (shape of the data between a slope of 1 and 0.75). In order to compare our results to Beladjine et al (2007) analysis, the figure 8 and 9 allows to determining the constants a, b, ay and by via linear fit. The parameters which best fit are summarized in Table 3 with the associated correlation coefficient. Even if the fit on figure 8 are good, the correlation coefficients are not because of the low dependence of e on the impact angle.

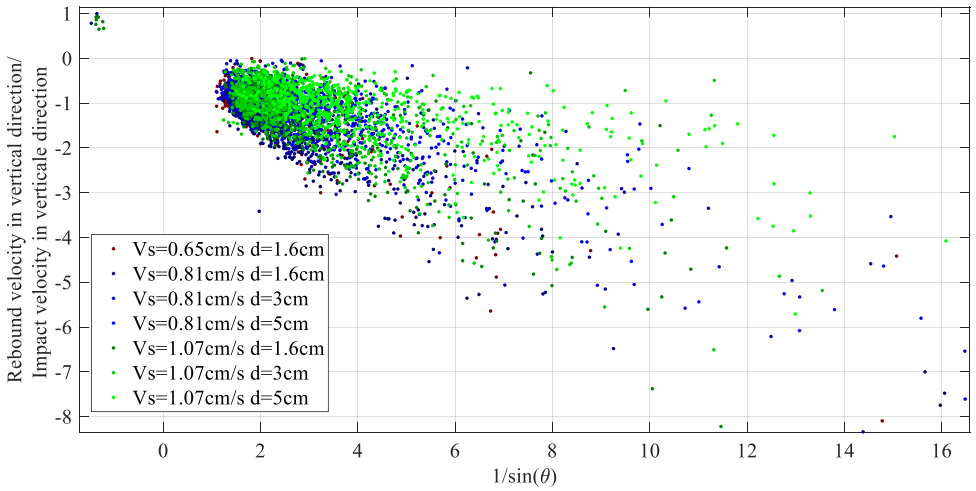

Figure 9. Determination of the coefficient of restitution a_y and b_y from the equation $Vimpact_y = -e_y \times Vrebound_y$ according to equation (7) for the seven configurations with different surface velocities Vs and particle diameters d

Table 3. Coefficient of restitution

Size of particle in movement (cm) d / Surface Velocity (m/s) Vs	e global coefficient $Vimpact/Vrebound$ (r^2)	e : $(a, b)(r^2)$	e_y : $(a_y, b_y)(r^2)$
Beladjine et al. (2007)	-	(0.87 ; 0.72)	(0.30 ; 0.15)
1.6 / 0.65	0.76 (0.72)	(0.88 ; 0.06) (0.01)	(0.51 ; -0.13) (0.99)
3 / 0.65	-	-	-
5 / 0.65	-	-	-
1.6 / 0.81	0.76 (0.69)	(0.98 ; 0.27) (0.15)	(0.42 ; -0.40) (0.91)
3 / 0.81	0.89 (0.74)	(0.98 ; 0.24) (0.18)	(0.28 ; -0.47) (0.90)
5 / 0.81	0.92 (0.72)	(0.98 ; 0.21) (0.16)	(0.27 ; -0.36) (0.85)
1.6 / 1.07	0.79 (0.80)	(0.87 ; 0.10) (0.03)	(0.52 ; 0.12) (0.98)
3 / 1.07	0.90 (0.94)	(0.95 ; 0.15) (0.04)	(0.59 ; 0.77) (0.99)
5 / 1.07	0.74 (0.43)	(0.97 ; 0.08) (0.01)	(0.29 ; 0.03) (0.75)
Mean	0.8244	(0.94 ; 0.16)	(0.41 ; -0.07)

Anyway we can notice an important difference between the experimental value that we obtain and the values used by Beladjine et al. (2007). Beladjine et al. (2007) presents a roughness resulting from jumps over an erodible bed made of same size particles. In this experimental simulation the bed is rigid and the roughness is smaller than the saltated particle diameters. A rigid bed is potentially less dissipative than an erodible bed leading to a bigger coefficient a. The observed differences seem coherent with this explanation.

The coefficient ay and by corresponding to the formula for the ratio between the rebound and impact vertical velocities are of the same order ((0.87; 0.72) for Berzi et al. (2016) and (0.94; 0.16) for the experimentation). Still the slope is weak but the dependency to theta is more visible with the vertical velocities. For a θ close to $\pi/2$ ($1/\sin(\theta)$ close to one), the magnitude of the velocity correspond almost to the vertical velocity and the ratio is then inferior to one between the incident and rebound velocity. For a more horizontal impact, the restitution in vertical is bigger than one, reaching even a factor of 5 for an angle with the horizontal of 4°.

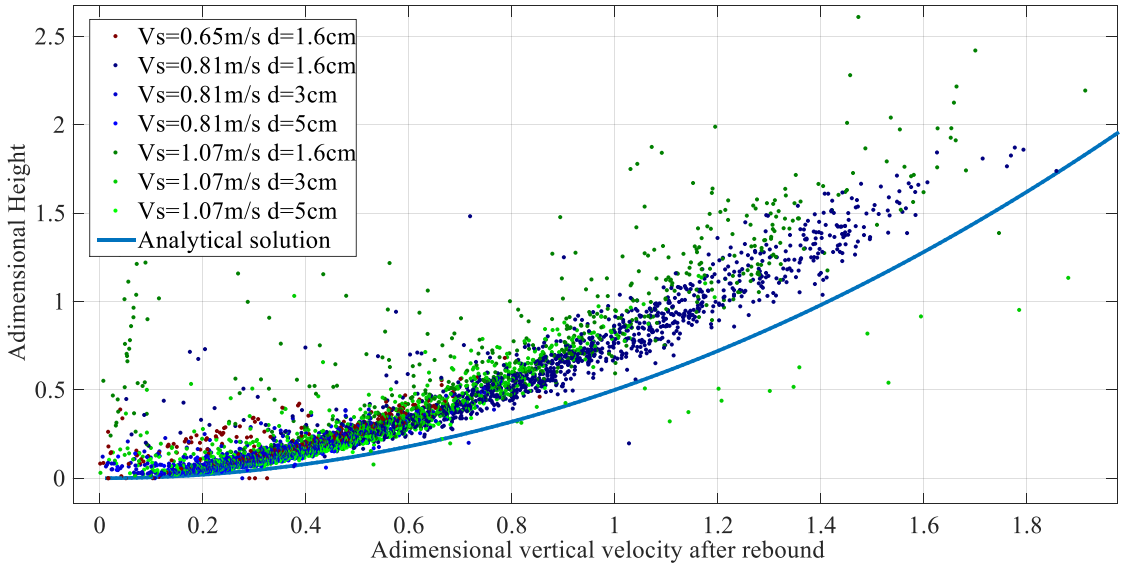

Figure 10. Trajectory height vs take off velocity obtains from the experimental data for the seven configurations with different maximal velocities Vs and particle diameters d; bold line represents the analytical solution if considering only weight acting on the particle

Figure 10 represents the dimensionless jump height H/d vs the dimensionless vertical component of the rebound velocity:

$$Vrebound_y/\sqrt{gd(\sigma-1)/\sigma}. \tag{8}$$

Analytically, considering only the weight force acting on the particles, the solution is

$$\frac{H}{d}=\frac{1}{2}\left(\frac{V_y}{\sqrt{gd(\sigma-1)/\sigma}}\right)^2 \tag{9}$$

Drag forces act against the particles velocities thus the height should be inferior to this maximal height if only considering drag. However, experimentally, the height of jumps is always higher than this analytical solution. That means that other forces act on the particle, in the direction opposed to the drag, contributing to increase the jump height. The inertia (added mass force) and the Magnus force due to the particle rotation could play an important role.

4. Discussion and conclusions

In this study, saltation regime is investigated for high Stokes number (inertial regime) experimentally. Two different motion regimes are observed: rolling and saltation. Rolling ratio is estimated experimentally from the length covered by the particle in rolling regime. 100% means no saltation observed, 0% means only saltation. If considering intermittent regime is between 75% to 25% of rolling ratio, the boundary with saltation regime (for 25% or less rolling movement) is about a Shield number of 0.1 for Stokes number between 10^4 and 10^5. Besides, the height of jumps is shown to be always superior to the maximum analytical height reached when considering only the weight force. This means that in reality, inertia and lift forces contributes to the ascendant part of the trajectory. Added mass and lift (Magnus) forces may play an important role in saltation, contributing to a better flight of the spherical particles. Actually, the particles have been observed to rotate at a rotation speed about 15 rad/s (for 5 cm diameter particles). The added

mass for a sphere into water is equivalent to half its mass. Considering an approximation for the estimation of Magnus force (for a smooth rotating ball in aeolian environment):

$$F \approx (\pi(d/2)^3 \rho^f)\omega V \tag{10}$$

With V the particle velocity and ω the the angular velocity. Using the rebound velocities, and mean acceleration during ascendant trajectory lead to an estimation of each force acting on the particles:

Table 4. Comparison of estimated mean forces acting on the saltating particles

Diameter	Weight	Lift (Magnus Force)	Drag	Added mass
1.6 cm	P1=0.05 N	20% P1	20% P1	20% P1
5.0 cm	P2=1.60 N	25% P2	13% P2	8% P2

According to these estimations (Table 4), the lift has the same order of magnitude than the drag and the added mass. These two forces must be taken into account in order to simulate the maximum height possibly reached.

A comparison is performed to the numerical model proposed by Berzi et al. (2016) and Jenkins & Valance (2014). The model solves the fundamental principle of dynamics on spherical spheres of uniform mass and diameter. Periodic solutions are investigated considering only weight and drag as forces acting on the particles. A steady saltation regime is reached or not according to the fixed conditions: particles diameter, flow current, restitution coefficients between the impact and the rebound velocities, particles flux. The aim of this model is to investigate the boundary of intermittent and saltation regime in condition comparable to extreme tidal current conditions. In this purpose Stokes number from 10^4 to 10^5 are considered. The vertical mass flux is taking low enough to simulate no interaction between the particles (few particles per $m^{-2}.s^{-1}$). Numerical results are presented on figure 11 for diameter from 0.1 to 19 cm and current velocities from 10 to 300 cm/s. Dots stand for conditions leading to a periodic saltation regime and crosses stand for conditions leading to a not-converged result. No saltation regime is deduced from a convergence issue between the model and a physical result (crosses). A transition zone between saltation or no saltation appears (grey part on figure 4) for a Shields number of 0.2.

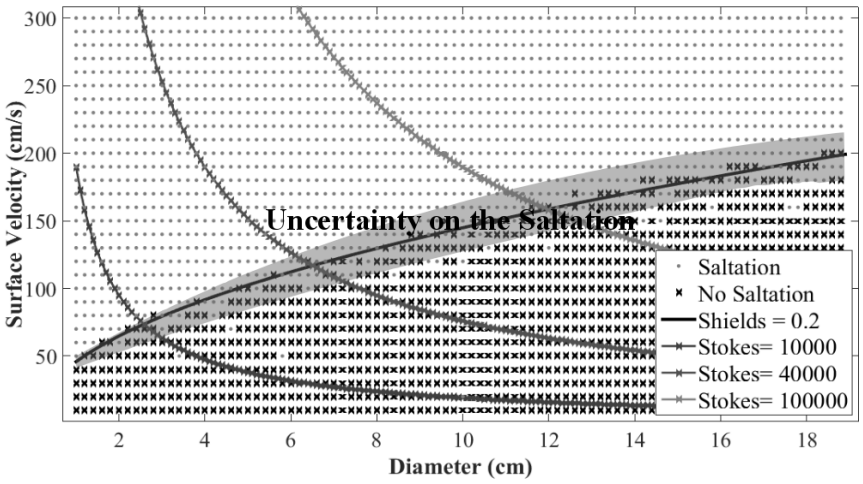

Figure 11. Simulation of periodic saltation adapted from Berzi and al. (2016) method. Parameters: density ratio 2.8; fluid kinematic viscosity 0.0014 $cm^2.s^{-1}$

The numerical transitional regime boundary is coherent with the transitional regime boundaries found experimentally. However the numerical height is lower than the analytical maximum height if considering only the weight of the particle by construction of the numerical model.
The inertia and lift forces does not seem to play an important role on the transition to saltation regime but may be primordial in order to fit the real jump characteristics such as length and height of the jump. A more detailed comparison between the numerical and experimental trajectories is carried out. Further investigations could be done by implementing the added mass in the numerical method. The possibility of implementing the Magnus forces in Berzi et al. (2016) model is currently evaluated. Further investigations are currently done on the experimental results. Two other roughnesses have been tested and must be processed.

Acknowledgements

The work is supported by the project ANR FEM PHYSIC ANR-10-IEED-0006-10. The authors want to give a special thanks to IPR team for their help during the lab experiment.

References

Berzi, D., Jenkins, J.T., Valance, A. (2016). *Periodic saltation over hydrodynamically rough beds: aeolian to aquatic.* Journal of Fluid Mechanics, Vol. 786, pp 190-209.
Beladjine, D., Ammi, M., Oger, L., & Valance, A. (2007). Collision process between an incident bead and a three-dimensional granular packing. *Physical Review E*, *75*(6), 061305.
Blanpain, O., 2009. *Dynamique sédimentaire multiclasse: de l'étude des processus à la modélisation en Manche.* Thèse de Doctorat, Université de Rouen.
Crassous, J., Beladjine, D., & Valance, A. (2007). Impact of a projectile on a granular medium described by a collision model. *Physical Review Letters*, *99*(24), 248001.
Durán, O., Andreotti, B. and Claudin, P., 2012. *Numerical simulation of turbulent sediment transport, from bed load to saltation.* Phys. Fluids Vol. 24, pp 1–17.
Foerster, S. F., Louge, M. Y., Chang, H., & Allia, K. (1994). Measurements of the collision properties of small spheres. *Physics of Fluids*, *6*(3), 1108-1115.
Gondret, P., Lance, M., & Petit, L. (2002). Bouncing motion of spherical particles in fluids. *Physics of Fluids*, *14*(2), 643-652Van Rijn(1984)
Jenkins, J.T. and Valance A., 2014. *Periodic trajectories in aeolian sand transport*. Physics of Fluids, Vol. 26(7).
Joseph, G. G., Zenit, R., Hunt, M. L., & Rosenwinkel, A. M. (2001). Particle–wall collisions in a viscous fluid. *Journal of Fluid Mechanics*, *433*, 329-346.
Niño, Y., & García, M. (1998). Experiments on saltation of sand in water. *Journal of Hydraulic Engineering*, *124*(10), 1014-1025.
Oger, L., Ammi, M., Valance, A., & Beladjine, D. (2005). Discrete element method studies of the collision of one rapid sphere on 2D and 3D packings. *The European Physical Journal E: Soft Matter and Biological Physics*, *17*(4), 467-476.
Soulsby R.L., 1997. *Dynamics of Marine Sands: a manual for practical applications*. Thomas Telford, London, ISBN 0-7277-2584-X.
Van Rijn, L. C. 1984. Sediment transport, part I: bed load transport. *Journal of hydraulic engineering*, *110*(10), 1431-1456.
Van Rijn, L. C. (1993). *Principles of sediment transport in rivers, estuaries and coastal seas* (Vol. 1006). Amsterdam: Aqua publications.
Williams, J.J., 1990. *Video observations of marine gravel transport*. Geo-Marine Letters, Vol. 10, pp 157–164. , Vol. 10, pp 157–164.